AD-A194 003 AN ASSESSMENT OF THE DRAG REDUCTION PROPERTIES OF DIDLETS AND THE PENALT.. (U) ROYAL AIRCRAFT ESTABLISHMENT FARNBOROUGH (ENGLAND) L GAUDET AUG 87 1/1

UNCLASSIFIED RAE-TM-2113 DRIC-BR-104024 F/G 1/1 NL

[redacted]

END
DATE FILMED
8 88
DTIC

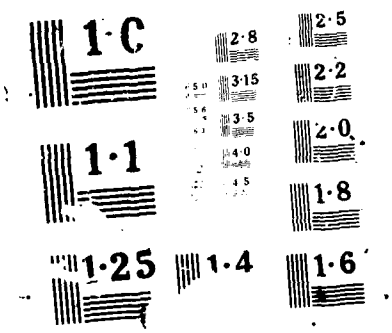
1·C
2·8
2·5
3·15
2·2
3·5
2·0
1·1
4·0
1·8
1·25
1·4
1·6

TECH. MEMO
AERO 2113

TECH. MEMO
AERO 2113

(2)

ROYAL AIRCRAFT ESTABLISHMENT

AN ASSESSMENT OF THE DRAG REDUCTION PROPERTIES OF RIBLETS AND THE PENALTIES OF OFF-DESIGN CONDITIONS

by

L. Gaudet

August 1987

Procurement Executive, Ministry of Defence
Farnborough, Hants

R O Y A L A I R C R A F T E S T A B L I S H M E N T

Technical Memorandum Aero 2113

Received for printing 4 August 1987

AN ASSESSMENT OF THE DRAG REDUCTION PROPERTIES OF RIBLETS AND THE PENALTIES OF OFF-DESIGN CONDITIONS

by

L. Gaudet

SUMMARY

An assessment is given of the performance of riblets in reducing skin friction in turbulent flow. The data of Sawyer and Winter is used to develop skin-friction relationships derived from the velocity profile for a turbulent boundary layer as modified by a riblet surface. The maximum percentage drag reduction is shown to vary with Reynolds number R_x . At large values of the non-dimensional riblet height the riblet surface acts as a uniform roughness and a value for the equivalent sand-grain roughness height is given. Examples of the estimated drag reductions which might be achieved for two current aircraft by incorporating riblet surfaces are presented.

LIST OF CONTENTS

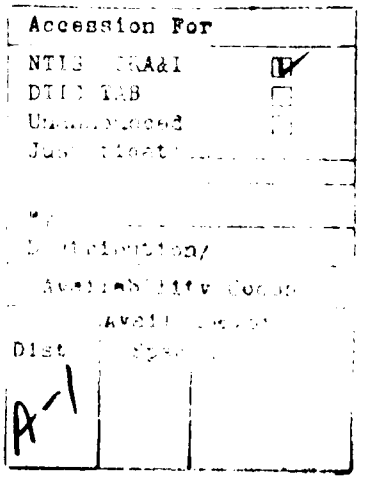

1 INTRODUCTION

The prospect of significant savings in fuel and improved performance for many forms of air and water-borne transport has stimulated interest in devices for manipulating the structure of turbulent boundary layers with the objective of reducing skin friction. Of the various methods[1] which have been tried the case for riblets (small streamwise surface grooves) appears to be well proven and with the use of composite structures they have the potential of being an integral-design feature by being moulded into the surface.

Measurements made at NASA[2] at low speed and zero pressure gradient have been confirmed at RAE by Sawyer and Winter[3] and show that reductions of 7-8% in skin friction may be achieved. If drag reduction is to be obtained, the grooves need to be sized to be within certain limits in terms of the viscous length scale characteristic of the region close to the wall and an optimum size for maximum drag reduction exists. For riblets whose size extends beyond the upper limit a drag increase will occur. Though this increment is small compared with that produced by sand-grain roughness, it is significant and thus needs to be quantified to assess the penalties to be paid at 'off-design' conditions.

An analysis is made here of the data of Sawyer and Winter covering both the drag reduction and the roughness aspects of riblets. The analysis is based on the fact that changes in surface texture modify the velocity profile in the wall region characteristically by a displacement of the logarithmic line. An analysis of the modified velocity profile leads to skin-friction relationships for a riblet surface and allows an estimate of the potential gains to be expected beyond the range of the experimental data.

This analysis is based on data obtained in zero pressure gradient flows at low speed. It is expected to be equally applicable to flows with streamwise pressure gradients and to high-speed flows with the use of suitable compressibility factors.

2 METHOD OF ANALYSIS

2.1 Modified velocity profile

The classical description of the velocity profile in a turbulent boundary layer is given by

$$\frac{u}{u_\tau} = \frac{1}{\kappa} \ln \frac{u_\tau y}{\nu} + \phi \left(\frac{y}{\delta}\right) \qquad (1)$$

where u is the velocity at a distance y from the surface,

u_τ = friction velocity
ν = kinematic viscosity
δ = boundary layer thickness
and κ = von Karman constant.

Hama[4] has shown that, for rough surfaces, the velocity is described by equation (1) with the addition of a term F which is a function of the surface roughness parameter $h^+ = u_\tau h/\nu$, where h is the height of the roughness. This property can be shown to be equally true for riblets of different geometry, as is demonstrated in Fig 1 for some sample profiles of Sawyer and Winter's data. These data include cases with both increase and decrease of surface shear relative to the smooth plate case where the velocity profile in the wall region is described by

$$\frac{u}{u_\tau} = \frac{1}{\kappa} \ln \frac{u_\tau y}{\nu} + \phi(0) \tag{2}$$

Here $\kappa = 0.41$ and $\phi(0) = 5.0$ and are the values which will be used in all subsequent analysis. The velocity profile is now represented by

$$\frac{u}{u_\tau} = \frac{1}{\kappa} \ln \frac{u_\tau y}{\nu} + F\left(\frac{u_\tau h}{\nu}\right) + \phi\left(\frac{y}{\delta}\right) , \tag{3}$$

and following an analysis similar to that given in Refs 5, 6 and 7 the relationship for the shape parameter remains the same as that for a smooth surface namely:

$$H = \frac{\delta^*}{\Theta} = \left(1 - \frac{G}{\lambda}\right)^{-1} , \tag{4}$$

where δ^* and Θ are the displacement and momentum thicknesses of the turbulent boundary layer and $\lambda = \sqrt{2/c_f}$ where c_f is the local skin-friction coefficient. The shape parameter $G = C_2/C_1$ is unaffected by the riblet surface since $C_1 = \int_0^1 \left(\frac{u_\delta - u}{u_\tau}\right) d(y/\delta)$ and $C = \int_0^1 \left(\frac{u_\delta - u}{u_\tau}\right)^2 d(y/\delta)$, where u_δ is the streamwise velocity when $y = \delta$ and both these quantities are unaffected by the function F in equation (3). The equation relating the local skin friction coefficient to the displacement thickness Reynolds number becomes

$$R_\delta^* = C_1 e^{-\kappa\phi(1)} e^{\kappa(\lambda - F)} . \quad (5)$$

Since it follows from the foregoing analysis that G and $C_1 e^{-\kappa\phi(1)}$ are unchanged by the surface geometry, their respective values of 7.0 and 0.158 have been taken from the smooth wall data ($F = 0$). The value of F may now be obtained from equation (5) knowing R_δ^* and the skin-friction coefficient. Plots of F versus $h^+ = u_\tau h/\nu$ are shown in Fig 2a for the four riblet tested. The data for the two cusped riblet surfaces, which are of similar shape, show good agreement. The data for the two V-shaped riblet surfaces indicate that the variation of F with h^+ is different from that for the cusped riblet and that a difference is apparent between the two V-groove riblets due to their different cross sections. If however a parameter $s^+ = u_\tau s/\nu$ is used, where s is the spacing between the peaks of the grooves, it appears that a correlation is obtained for all riblet geometries for positive values of F, as shown in Fig 2b, and a maximum value exists for F of about 1.0. These results suggest that, for drag reduction, the dominant dimension is the spacing between the riblet peaks which may act as tramlines and have a restraining influence on the streamwise vortex flow in the wall region of the boundary layer. While Fig 2b clearly shows that an optimum value exists for s^+ of about 15, there is also a suggestion that the larger aspect ratio s/h may have the effect of extending the upper limit of s^+ for which F remains positive. When $F < 0$ the riblets act as a uniformly distributed roughness and the condition for fully-developed roughness flow is rapidly approached with increasing s^+, as indicated by the slopes of the curves in Fig 2. For rough surfaces it is normal[8] to represent the velocity profile in the law-of-the-wall region by

$$\frac{u}{u_\tau} = \frac{1}{\kappa} \ln \frac{y}{h} + g(h^+) , \quad (6)$$

which allows the parameter g to be determined from the velocity profile in the wall region. Equally, g may be determined by comparing equations (3) and (6) for the wall region to give

$$g(h^+) = \frac{1}{\kappa} \ln h^+ + F(h^+) + \phi(0) . \quad (7)$$

The values for g for the data of Sawyer and Winter as determined from equation (7) are shown in Fig 3. A line corresponding to the smooth surface (ie, for $F = 0$) is shown in Fig 3 together with a curve representing Nikuradse's data[9] for sand-grain roughness for which values of 0.4 and 5.5 were used for κ and $\phi(0)$, respectively.

2.2 Skin-friction relationships for a riblet surface

When a relationship such as that shown in Fig 2 for the parameter F is known, the appropriate skin-friction laws may be determined for a riblet surface.

From equations (4) and (5), the Reynolds number based on momentum thickness becomes

$$R_\Theta = \alpha \lambda \left(-\frac{G}{\lambda}\right) e^{\kappa(\lambda - F)} , \tag{8}$$

where $\alpha = C_1 \, e^{-\kappa\phi(1)}$.

Equation (8) together with the momentum integral equation for zero pressure-gradient flow

$$\frac{C_f}{2} = \frac{1}{\lambda^2} = \frac{dR_\Theta}{dR_x} \tag{9}$$

allows the Reynolds number based on a streamwise length x to be determined in the form

$$R_x = \alpha \int_0^\lambda \kappa \lambda^2 \left(1 - \frac{dF}{d\lambda}\right)\left(1 - \frac{G}{\lambda}\right) e^{\kappa(\lambda - F)} d\lambda \tag{10}$$

which then permits the mean skin-friction coefficient to be determined from

$$C_F = \frac{1}{x}\int_0^x c_f dx = \frac{2R_\theta}{R_x} \tag{11}$$

Since the V-shaped riblet with $s/h = 2$ produces the least drag of all the surfaces studied by Sawyer and Winter, the data for this case have been chosen for computation. Curves were fitted to the data thus allowing solutions to be obtained to equations (8), (10) and (11). The integral in equation (10) was

determined numerically. The results are shown in Figs 4 and 5 for both local and mean skin-friction coefficient plotted against the appropriate Reynolds number for various values of R_h, the Reynolds number based on the riblet height h. Also shown are the relationships for a smooth surface ($F = 0$) and an optimised surface, ie, one where the riblet height is varied along the surface so that the maximum drag reduction condition $s^+ = 15$ is achieved over the complete surface. For the case when F has a constant value equation (9) may by integrated analytically to give

$$R_x = \alpha\left[\lambda^2 - \lambda\left(\frac{2}{\kappa} + G\right) + \frac{2}{\kappa}\left(\frac{1}{\kappa} + G\right)\right]e^{\kappa(\lambda-F)} \quad . \tag{12}$$

This is the skin-friction relationship for a smooth surface with Reynolds number factored by $e^{-\kappa F}$ or for the optimised surface ($F = 1$) by $e^{-\kappa}$. In Fig 5 it can be seen that, at best, a drag reduction of 7% may be achieved at $R_x = 10^6$ which is consistent with the experimental data while at higher Reynolds numbers the reduction in drag is less such that at $R_x = 10^9$ the reduction is about 5%. As is apparent in Figs 4 and 5, the skin-friction curves for $R_h = 200$ lie close to the optimum curves. This arises because, in the range $10^6 < R_x < 10^9$ of Figs 4 and 5, s^+ is in the range 10 to 20 and, as is evident in Fig 2b, the variation of F within this range of s^+ is small. For the values of $R_h > 200$ shown in Figs 4 and 5 the optimum drag reduction occurs at increasingly higher Reynolds numbers and beyond the range shown. At a given Reynolds number increase in R_h increases the skin-friction coefficient until values greater than that for a smooth surface are reached after which the riblets may be considered as producing a rough surface.

A measure of the roughness drag of riblets may be obtained from Fig 6 in which the mean skin-friction coefficient is shown plotted against R_x for a range of values of x/h. Beyond the region indicating a drag reduction, C_F is virtually constant for a fixed value of x/h which is typical of a fully developed roughness flow described by $g(h^+) = \text{constant}$.

With the aid of equations (7) and (8) equation (10) may be integrated analytically to give

$$\frac{x}{h} = \alpha A\left\{\left(\lambda - G - \frac{2}{\kappa}\right)e^{\kappa\lambda} + 2G\left(\ln\lambda + \kappa\lambda + \frac{(\kappa\lambda)^2}{2.2!} + \frac{(\kappa\lambda)^3}{3.3!} \ldots\right)\right\} \tag{13}$$

and

$$C_F = \frac{2\alpha A h}{\lambda x}\left(1 - \frac{G}{\lambda}\right)e^{\kappa\lambda} \tag{14}$$

where

$$A = e^{-\kappa(g(h^+) - \phi(0))} = 0.0443$$

for $g(h^+) = 12.6$, the asymptote for V-grooves with $s/h = 2.08$ taken from Fig 3. A plot of C_F versus x/h for fully developed roughness flows is shown in Fig 7. Comparison is made with the results for sand-grain roughness and it is seen that for the same mean skin-friction coefficient the height of the equivalent sand-grain roughness is one tenth of that of the riblet height.

3 APPLICATION TO AIRCRAFT CONFIGURATIONS

To apply the analysis to aircraft drag estimates suitable compressibility factors are required. For skin-friction relationships which are derived from a transformed velocity profile such as those by Winter and Gaudet[5] and Van Driest[10] the factors remain unchanged from those for a smooth surface.

Estimates have been made of the potential drag reduction for two current aircraft, the BAe 125 Executive Jet ($M = 0.7$ at 12500 m) and the A300 Airbus ($M = 0.8$ at 10000 m). The riblets have been sized to give drag reductions close to the optimium with riblet heights of 0.05 mm and 0.03 mm for BAe 125 and the A300 respectively. Any influence of streamwise pressure gradients upon riblet performance has been assumed to be negligible since the velocity profile as described by equation (2) is only weakly, if at all, affected by the pressure gradient. The estimates have been made using a simple strip technique, assuming zero pressure gradient flow, to determine the difference in skin friction produced by the riblets. The results are shown in Fig 8 as a reduction in the drag coefficient of $\Delta C_D = \Sigma \Delta C_F \cdot A/A_w$, where ΔC_F is the change in mean skin friction due to the riblet surface over the area A and A_w is the wing reference area. Reductions of 6.5×10^{-4} and 4.7×10^{-4} in C_D have been estimated for the BAe 125 and the A300 respectively which illustrates the greater benefits possible at lower Reynolds numbers. The reduced benefits of partial coverage of the wing, tail and fuselage have also been estimated with the riblet surface starting at distances 25% and 50% downstream of the leading edges and nose. While this arrangement would be expected to reduce the benefits in proportion to the area of the riblet surface, the values of ΔC_D shown in Fig 8 are less than this since the rearward areas are in a higher Reynolds number region where the drag reduction is less.

The application of riblets to the complete surface of an aircraft would need care to avoid the disadvantages of misalignment of the riblets at cruise

conditions. In the regions of the attachment line and the trailing edge of a swept wing, for example, where large variations in the the direction of the surface streamlines occur it may be difficult to align the riblets with the surface flow direction. Failure to do this may result in the riblets acting as a rough surface and it might be prudent to consider leaving such sensitive areas smooth. Similar problems might be expected at the front and rear of the fuselage. On the other hand the reduction in surface shear which is expected from a well-aligned riblet surface would slightly thin the boundary layer and this is expected to produce beneficial effects in flows with severe adverse pressure gradients (eg shock waves).

4 CONCLUSIONS

Analysis of the drag and velocity profile measurements of Sawyer and Winter has shown that, for drag reduction, the data correlate best in terms of the wall parameter s^+ based on the lateral spacing of the riblets for the riblet geometries considered.

For large values of the wall parameter when the riblet surface acts as a distributed roughness, resulting in a net drag increase, the geometry of the riblet becomes important. It appears that the V-shaped riblet with s/h = 2 has the least drag and its equivalent sand-grain roughness is one tenth of the riblet height for fully developed roughness flow.

The skin-friction relationships derived form the velocity profile as modified by the riblet surface show that for an optimum riblet size reductions in skin friction of about 7% may be achieved at $R_x = 10^7$ but that at $R_x = 10^9$ the reduction is about 5%. Applied to the BAe 125 and the A300, for example, the analysis implies maximum possible reductions in the drag coefficient C_D of 6.5×10^{-4} and 4.7×10^{-4} respectively. These savings will decrease if it is not feasible to apply the riblets in regions which are surface-flow sensitive.

LIST OF SYMBOLS

A area of an aircraft surface

A_w reference area of wing

C_1 $\int_0^1 \left(\frac{u_\delta - u}{u_\tau}\right) d\left(\frac{y}{\delta}\right)$

C_2 $\int_0^1 \left(\frac{u_\delta - u}{u_\tau}\right)^2 d\left(\frac{y}{\delta}\right)$

C_D overall drag coefficient of aircraft

ΔC_D reduction in overall drag coefficient $= \Sigma\, \Delta C_f \cdot \frac{A}{A_w}$

c_f local skin-friction coefficient

C_F mean skin-friction coefficient $= \frac{1}{x}\int_0^x c_f\, dx$

F displacement of the logarithmic line in the velocity law-of-the-wall due to a riblet surface

g sand-grain roughness parameter

G boundary-layer shape parameter C_2/C_1

h *height of riblet*

h^+ non-dimensional riblet height $\frac{u_\tau h}{\nu}$

H boundary-layer shape parameter $\frac{\delta^*}{\Theta}$

R_h Reynolds number based on riblet height h

R_x Reynolds number based on streamwise length x

R_{δ^*} Reynolds number based on displacement thickness δ^*

R_Θ Reynolds number based on momentum thickness Θ

s riblet spacing peak-to-peak

s^+ non-dimensional riblet spacing $\frac{u_\tau s}{\nu}$

u streamwise velocity in boundary layer

u_δ streamwise velocity at edge of boundary layer

u_τ friction velocity $= \sqrt{\frac{\tau}{\rho}}$

x streamwise distance

y distance from surface

α defined in equation (8)

δ boundary layer thickness

δ^* displacement thickness $\int_0^\delta \left(1 - \frac{u}{u_\delta}\right) dy$

Θ momentum thickness $\int_0^\delta \frac{u}{u_\delta}\left(1 - \frac{u}{u_\delta}\right) dy$

LIST OF SYMBOLS (concluded)

κ von Karman's constant

λ $u_\delta / u_\tau = \sqrt{2/c_f}$

ν kinematic viscosity

ρ density

τ surface shear

ϕ wake term

REFERENCES

No.	Author	Title, etc
1	P. R. Bandyopadhyay	Mean flow in turbulent boundary layers disturbed to alter skin friction. Journal of Fluid Engineering, Vol. No. 108, (1986), 127-140
2	M. J. Walsh A. M. Lindemann	Optimisation and application of riblets for turbulent drag reduction. AIAA-84-0347, (1984)
3	W. G. Sawyer K. G. Winter	An investigation of the effect on turbulent skin friction of surfaces with streamwise grooves. (to be published)
4	F. R. Hama	Boundary layer characteristics for smooth and rough surfaces. Trans Soc Naval Architects Marine Eng 62, (1954), 333-35
5	K. G. Winter L. Gaudet	Some recent work on compressible turbulent boundary layers and excrescence drag. RAE Technical Memorandum 1115, Paper 15 NASA SP-216, (1968).
6	K. G. Winter L. Gaudet	Turbulent boundary layer studies at high Reynolds numbers at Mach numbers between 0.2 and 2.8. ARC R&M 3712, (1970)
7	L. Gaudet	Experimental investigation of the turbulent boundary layer at high Reynolds numbers and a Mach number of 0.8. Aeronautical Journal Vol. No. 90, (1986), 83-94
8	A. D. Young J. H. Paterson	Aircraft excrescence drag. AGARD-AG-264, (1981)
9	J. Nikuradse	Strömungsgesetze in Rauhren Rohren, Forsch. Arb. Ing. Wes. No. 361, (1933)

REFERENCES (concluded)

No.	Author	Title, etc
10	E. R. Van Driest	Turbulent boundary layer in compressible fluids. Journal of the Aeronautical Sciences, Vol.18, No. 3, (1951), 145-160

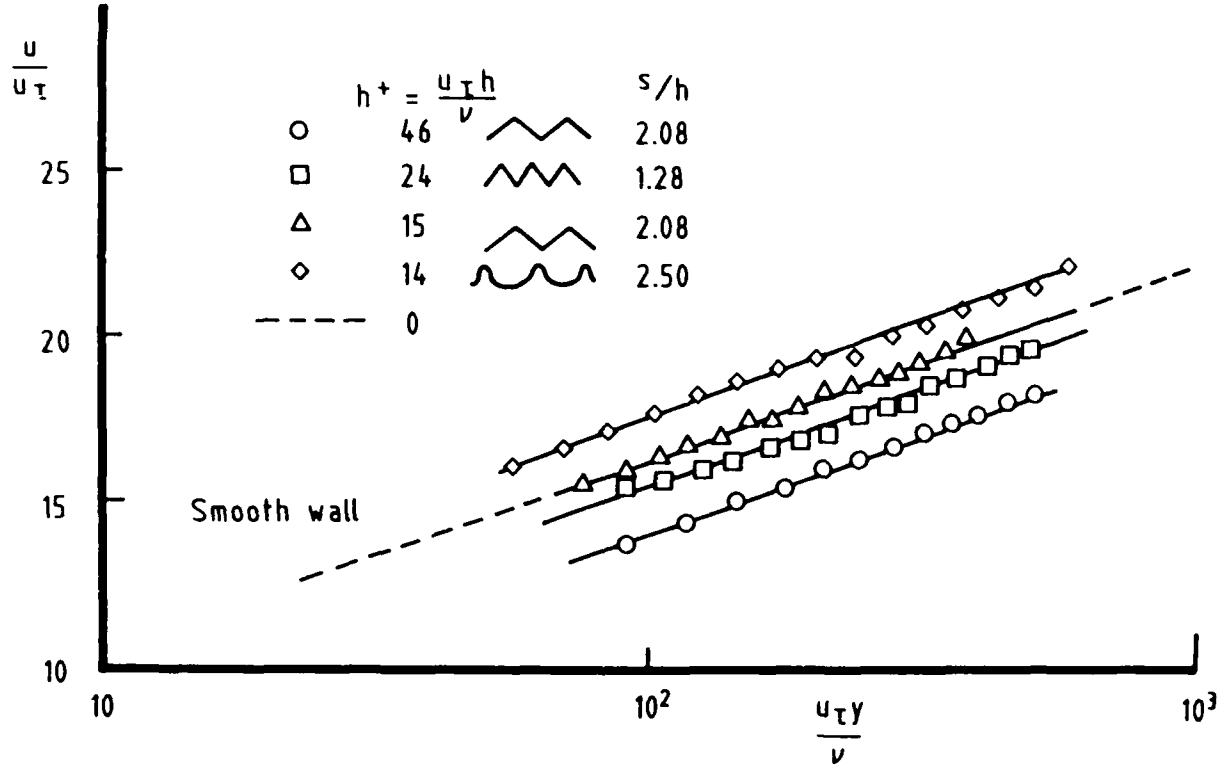

Fig. 1 Effect of riblets on the law-of-the-wall

Fig 2

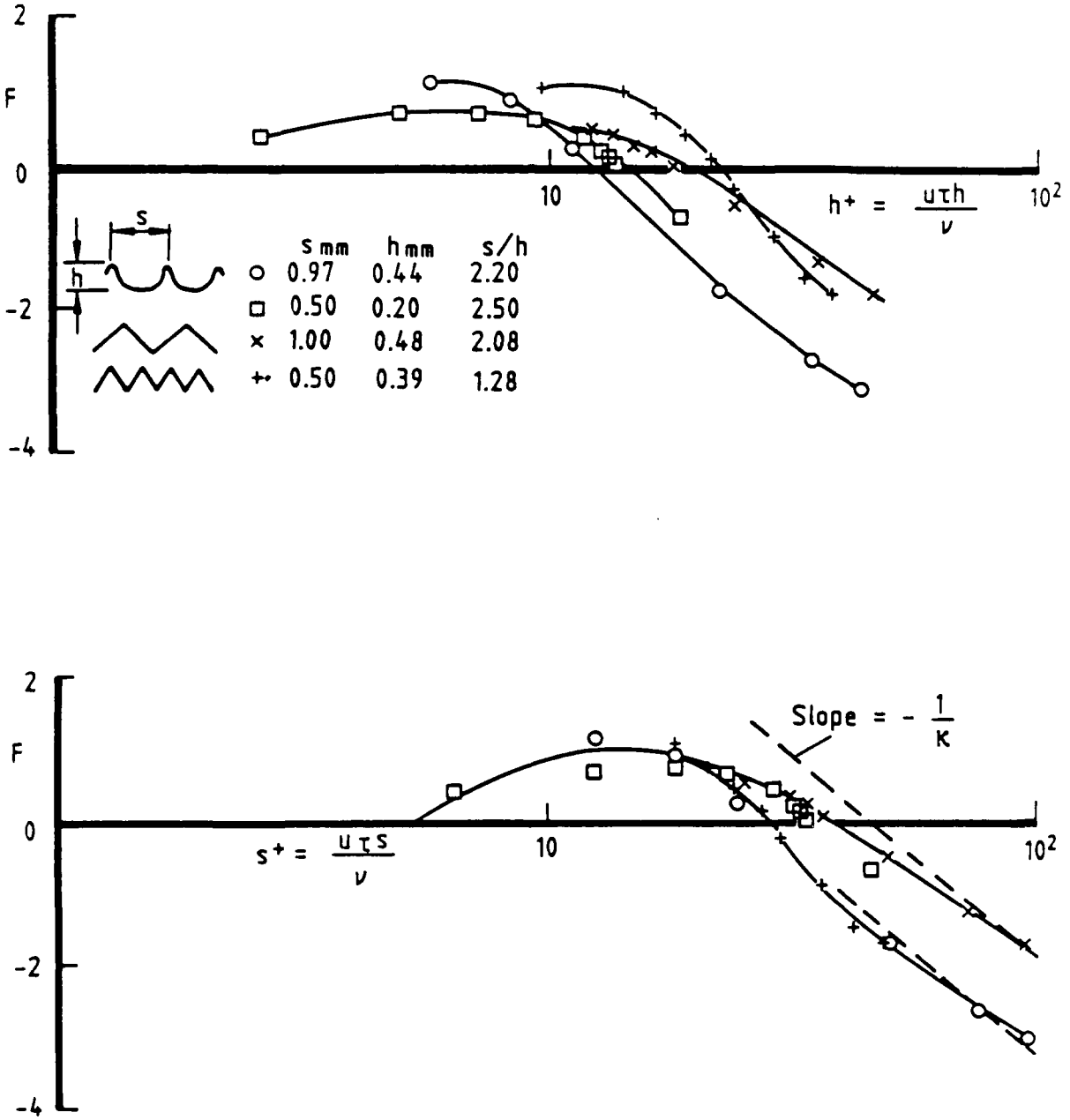

Fig. 2 Variation of F with roughness parameters

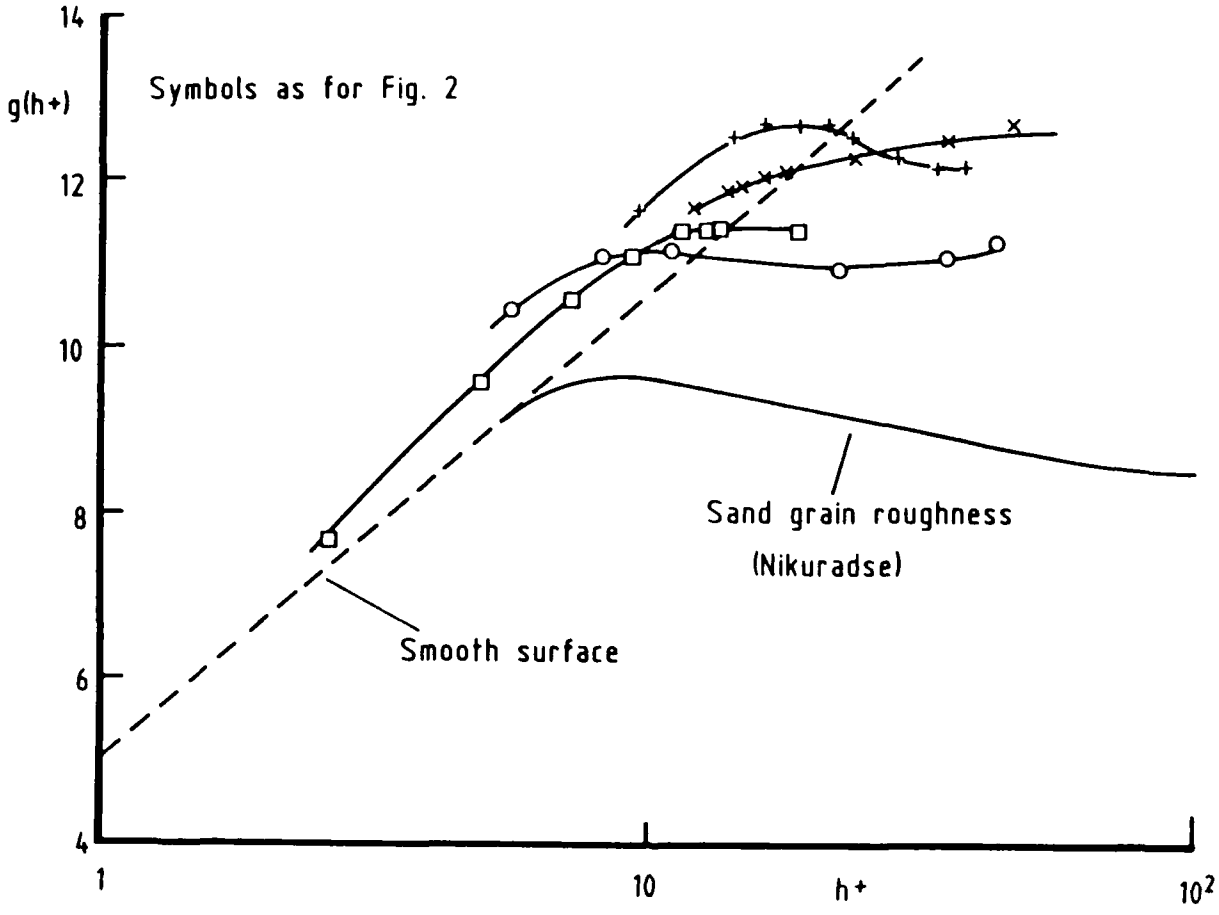

Fig. 3 Variation of roughness parameter g(h+) with h+

Fig 4

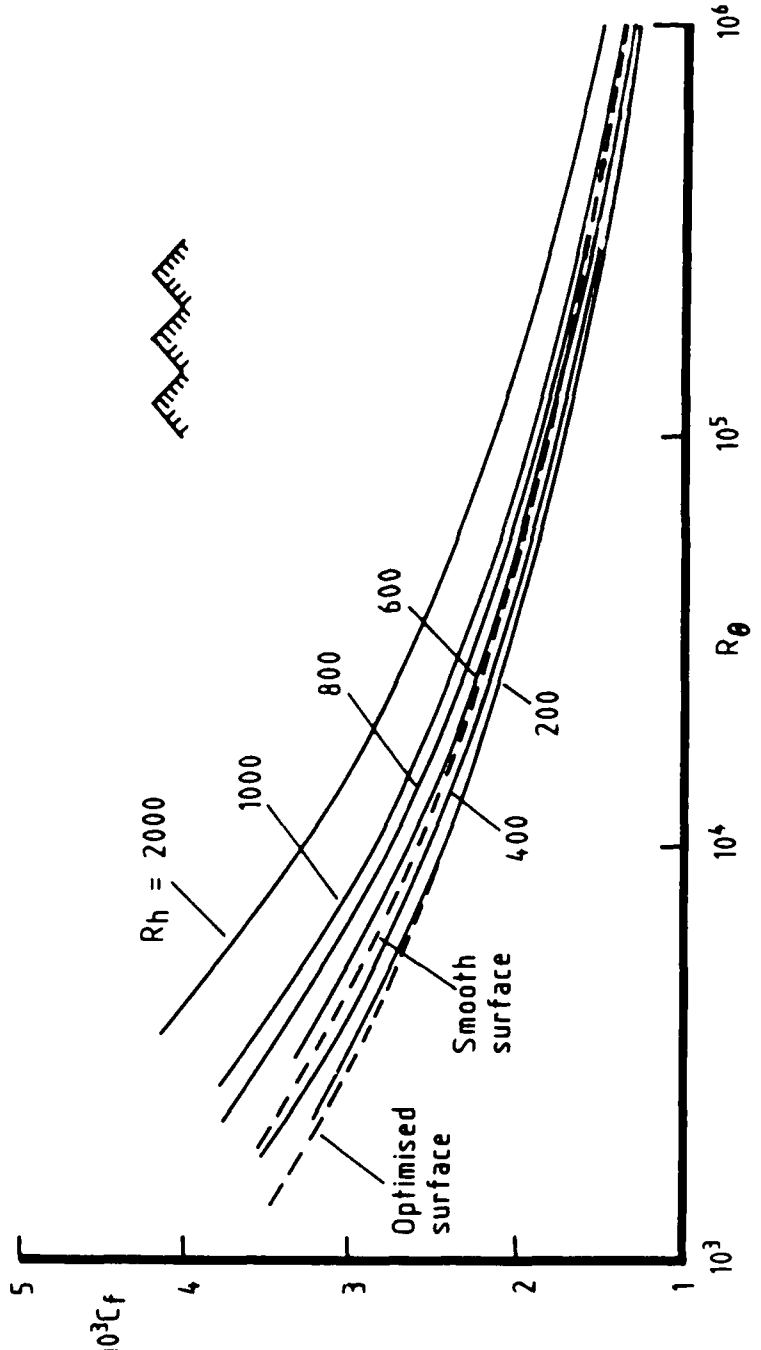

Fig. 4 Skin - friction relationship $C_f \sim R_\theta$

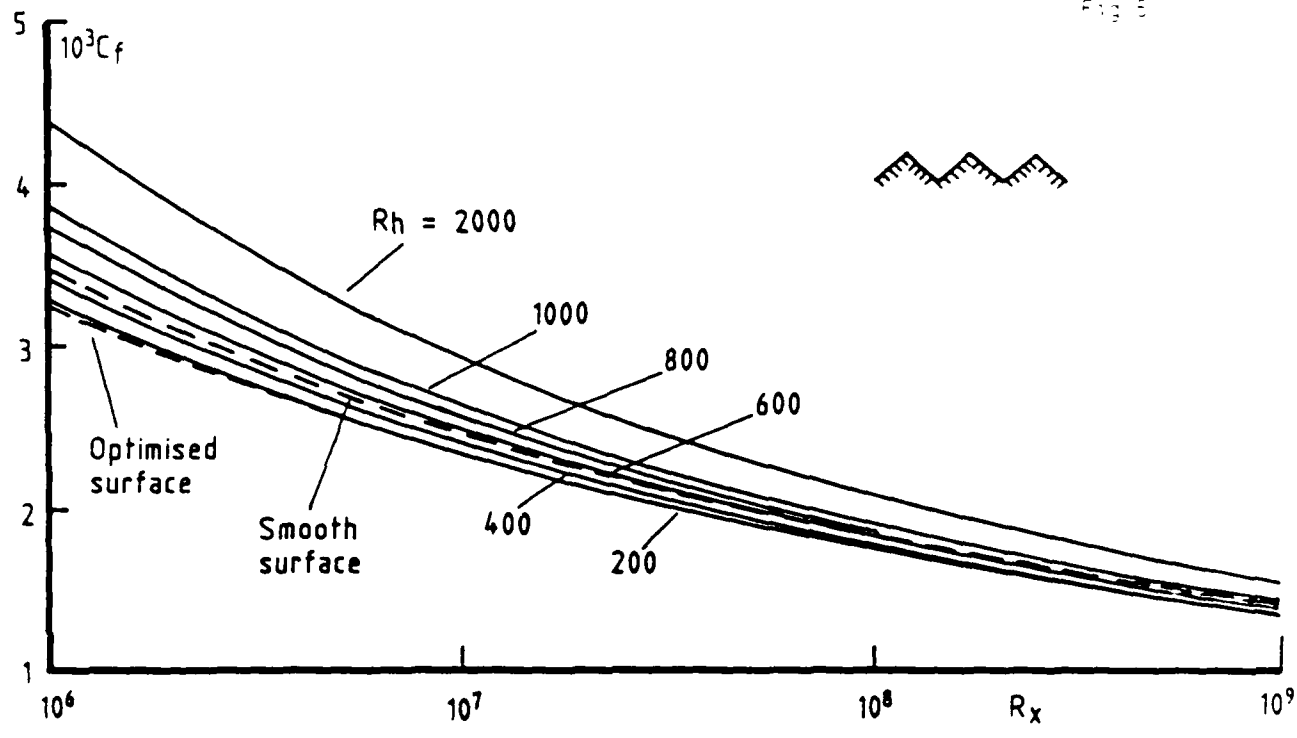

(a) Local skin friction coefficient

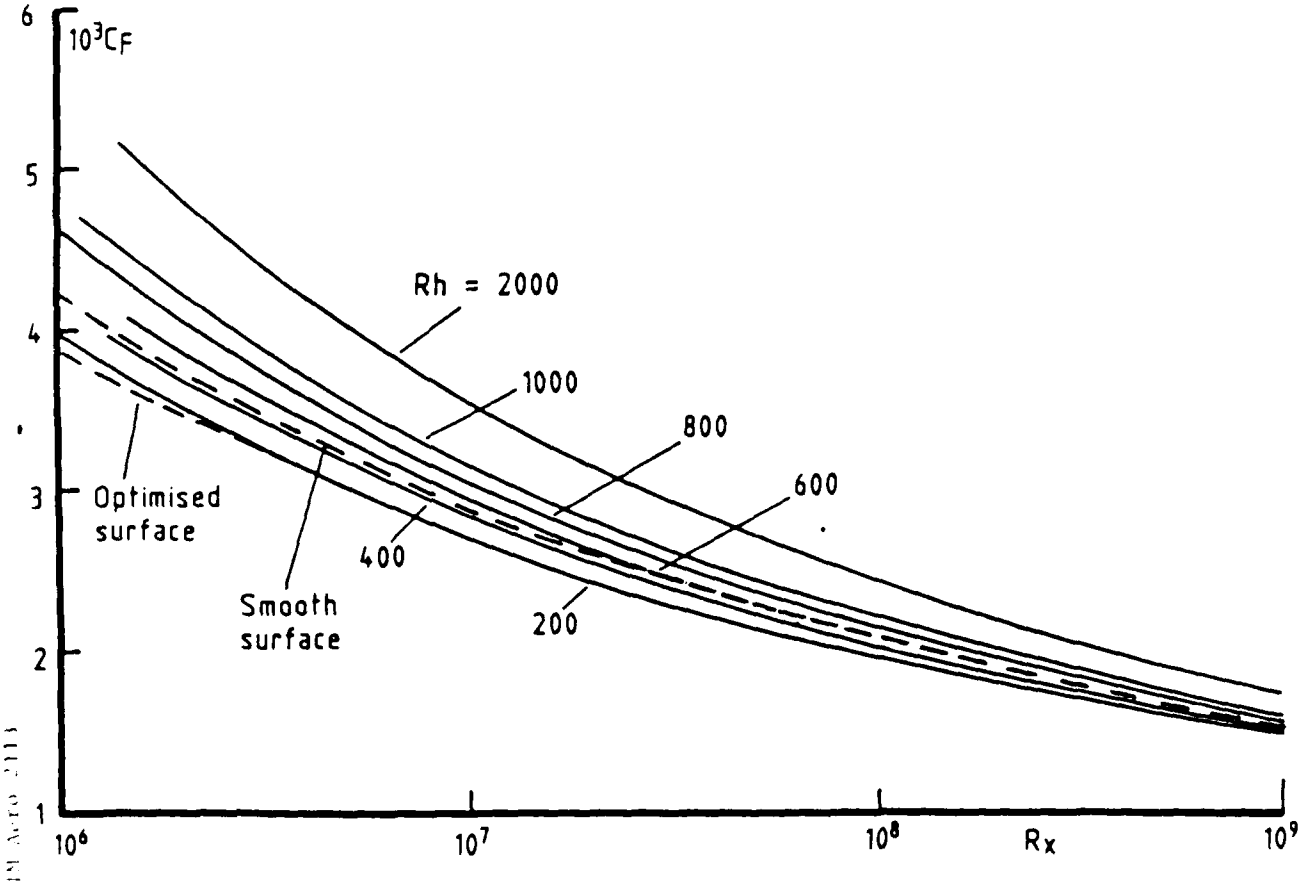

(b) Mean skin - friction coefficient

Fig. 5 Variation of skin friction with R_x

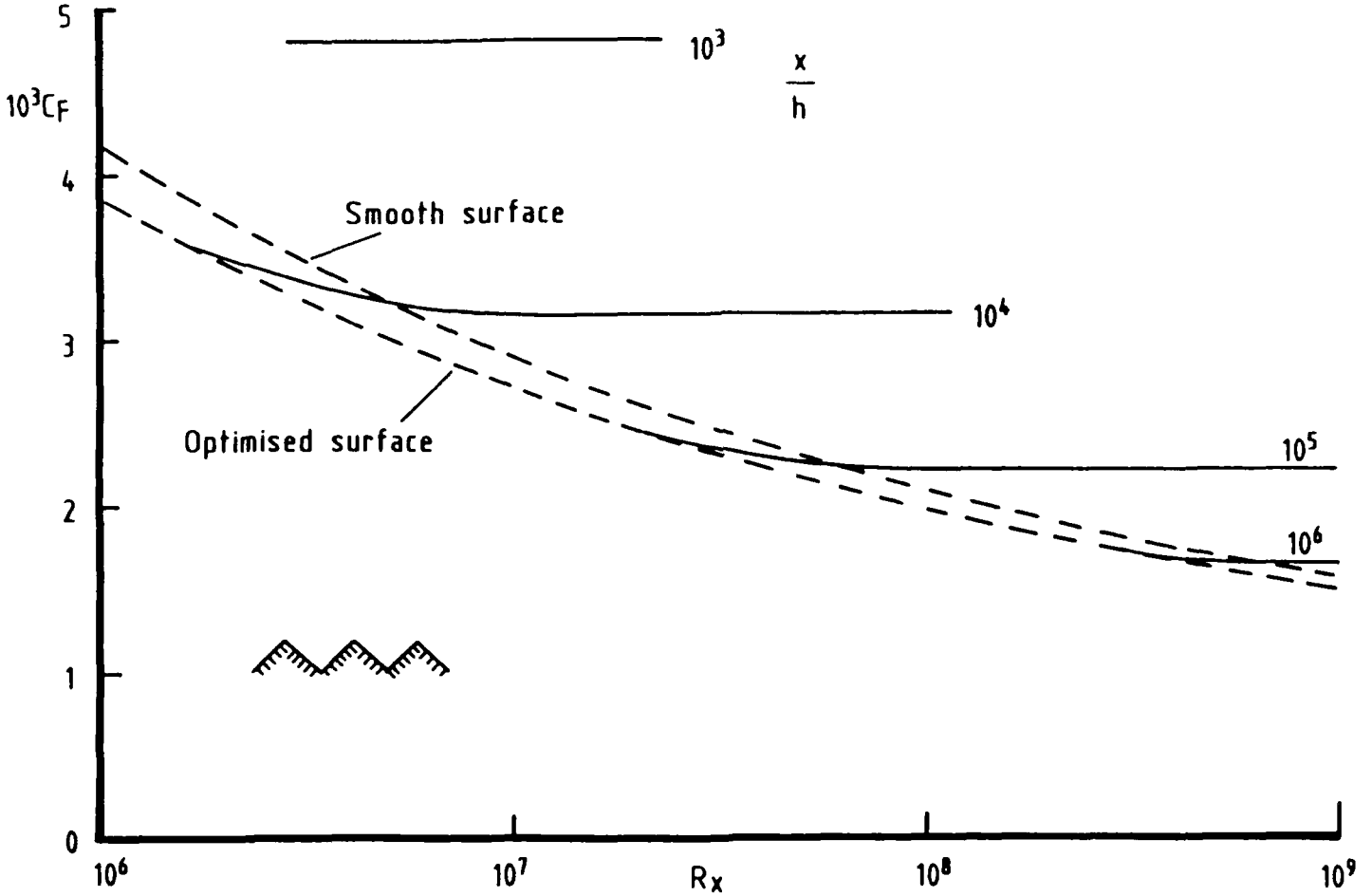

Fig. 6 Mean skin - friction coefficient for constant x/h

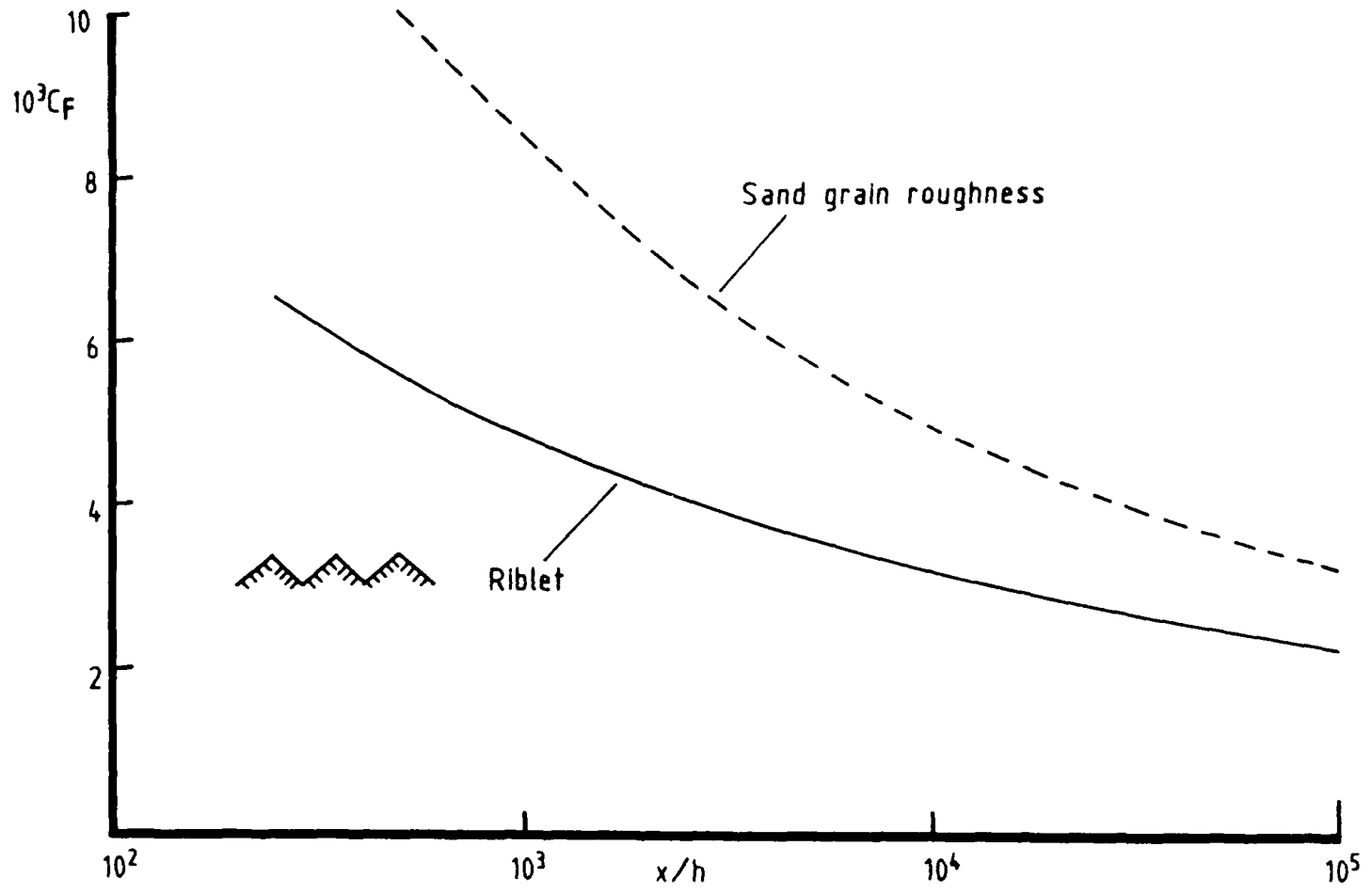

Fig. 7 Mean skin - friction coefficients for fully developed roughness flows

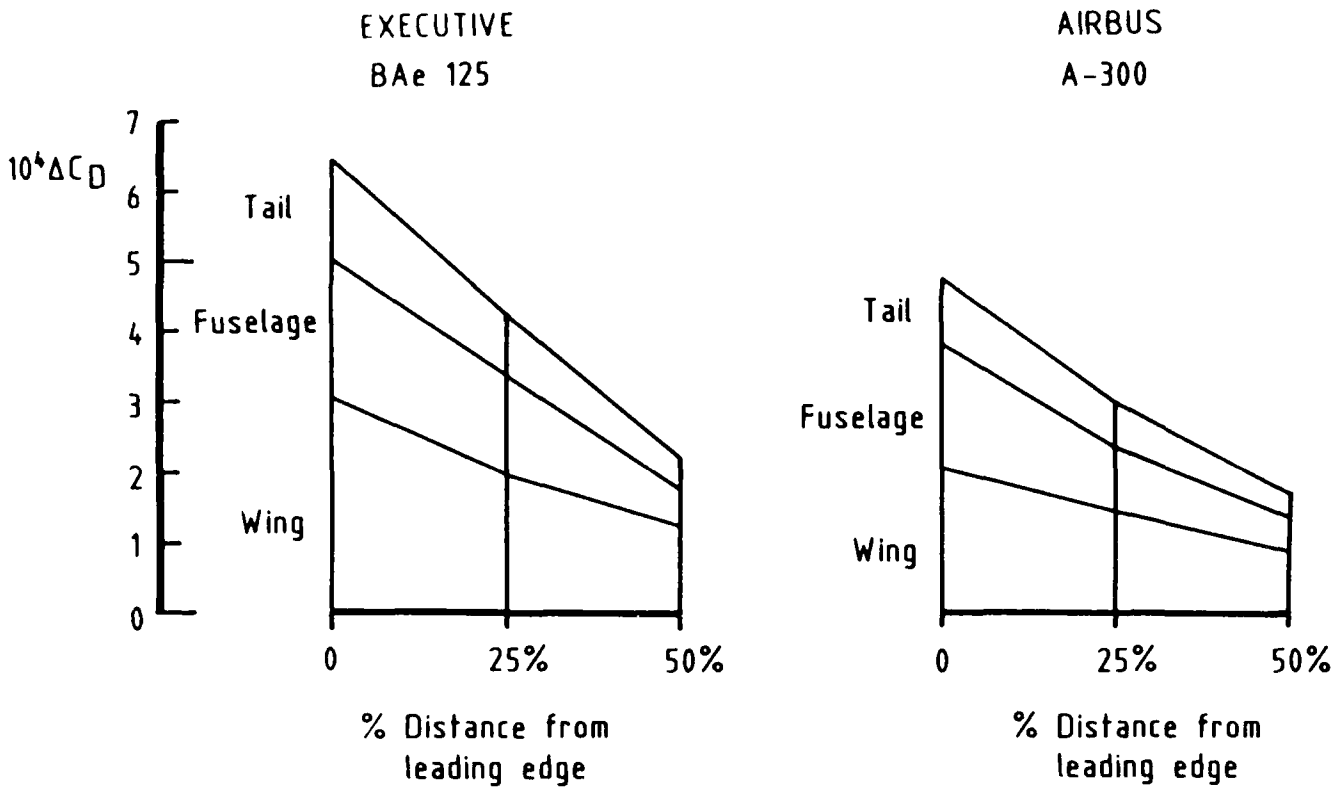

Fig. 8 Possible reductions in drag for two aircraft and effect of delaying the start of the riblet surfaces


TE
MED
8